ELSEVIER

Intermetallics 9 (2001) 25–31

Intermetallics

www.elsevier.com/locate/intermet

Processing and mechanical properties of a molybdenum silicide with the composition Mo–12Si–8.5B (at.%)

Joachim H. Schneibel [a,*], M.J. Kramer [b], Ö. Ünal [b], Richard N. Wright [c]

[a] *Oak Ridge National Laboratory, Metals and Ceramics Division, PO Box 2008, Oak Ridge, TN 37831-6115, USA*
[b] *Ames Laboratory, Iowa State University, Ames, IA 50011-3020, USA*
[c] *Idaho National Engineering and Environmental Laboratory, PO Box 1625, Idaho Falls, ID 83451-2218, USA*

Received 20 March 2000; accepted 25 May 2000

Abstract

Alloys with the nominal composition Mo–12Si–8.5B (at.%) were prepared by arc-melting or powder-metallurgical processing. Cast and annealed alloys consisted of approximately 38 vol.% α-Mo in a brittle matrix of 32 vol.% Mo_3Si and 30 vol.% Mo_5SiB_2. Their flexure strengths were approximately 500 MPa at room temperature, and 400–500 MPa at 1200°C in air. The fracture toughness values determined from the three-point fracture of chevron-notched specimens were about 10 MPa $m^{1/2}$ at room temperature and 20 MPa $m^{1/2}$ at 1200°C in air. The relatively high room temperature toughness is consistent with the deformation of the α-Mo particles observed on fracture surfaces. Three-point flexure tests at 1200°C in air and a tensile test at 1520°C in nitrogen indicated a small amount of high temperature plasticity. Extrusion experiments to modify the microstructure of cast alloys were unsuccessful due to extensive cracking. However, using powder-metallurgical (PM) techniques, microstructures consisting of Mo_3Si and Mo_5SiB_2 particles in a continuous α-Mo matrix were fabricated. The room temperature fracture toughnesss of the PM materials was on the order of 15 MPa $m^{1/2}$. © 2001 Elsevier Science Ltd. All rights reserved.

Keywords: A. Molybdenum silicides; B. Fracture toughness

1. Introduction

Molybdenum silicides such as $MoSi_2$ offer excellent oxidation resistance, but their fracture toughness tends to be low. The room temperature fracture toughness of $MoSi_2$ is only on the order of 3 MPa $m^{1/2}$ [1]. To improve room temperature fracture toughness and high temperature creep strength, a composites approach such as that pursued by Hebsur [1] is required. In that work, composites of $MoSi_2$ containing SiC fibers and Si_3Ni_4 particles were explored, and room temperature fracture toughness values up to 35 MPa $m^{1/2}$ were measured. However, the toughening mechanisms in these brittle–brittle composites are not based on energy absorption by the deformation of ductile phases, but rather on processes such as crack bridging, frictional energy dissipation during fiber pull-out, and crack deflection. Molybdenum silicides with silicon concentrations lower than those of $MoSi_2$ suffer from poor oxidation resistance. However, boron additions appear to alleviate the oxidation problem. As early as 1957, Nowotny et al. [2] pointed out that boron-containing silicides possess high oxidation resistance due to the formation of protective borosilicate glass. A slightly revised version of Nowotny's Mo–Si–B ternary phase diagram based on the work of Nunes et al. [3] is shown in Fig. 1. The range of stoichiometry of the Mo_5Si_3–B phase at 1800°C was also investigated in considerable detail by Huebsch et al. [4]. As compared to Nunes et al., they found the Mo_5Si_3–B phase to be closer to its stoichiometric composition, with a narrower homogeneity range in Si, and a higher B concentration. Based on Nowotny et al.'s work, boron-containing molybdenum silicides based on Mo_5Si_3 were recently developed at Ames Laboratory [5,6]. These silicides consist of approximately 25 vol.% Mo_3Si, 50 vol.% Mo_5Si_3 (T1), and 25 vol.% Mo_5SiB_2 (T2). Boron addition increased the oxidation resistance of Mo_5Si_3 by 5 orders of magnitude to a level near that

* Corresponding author. Tel.: +1-856-576-4644; fax: +1-865-574-7659.

E-mail address: schneibeljh@ornl.gov (J.H. Schneibel).

0966-9795/01/$ - see front matter © 2001 Elsevier Science Ltd. All rights reserved.
PII: S0966-9795(00)00093-5

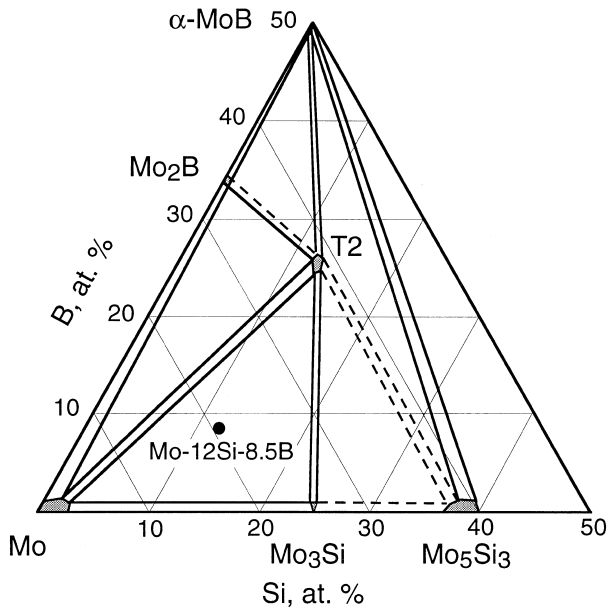

Fig. 1. Schematic section of the 1600°C isothermal ternary Mo–Si–B phase diagram after Nunes et al. [3].

of $MoSi_2$ in the temperature range 800–1300°C [5–7]. However, these silicides are brittle.

One way to toughen silicides is by the incorporation of ductile Mo. For example, brittle Mo_3Si may be toughened by Mo inclusions. Its oxidation resistance can be improved by boron additions. The resulting class of Mo–Si–B alloys was developed by Berczik [8,9] and consists of α-Mo (i.e. the Mo–Si–B solid solution), Mo_3Si, and Mo_5SiB_2. The phase relationships in these alloys have been studied recently by Perepezko and co-workers [3,10,11]. While their oxidation resistance is inferior to that of the Mo_3Si–T1–T2 alloys [12], it is likely that it can be improved by minimizing the α-Mo volume fraction, by suitable alloying additions, and/or by silicide coatings.

The purpose of the present work is to investigate the processing and microstructure of Mo–12Si–8.5B[1], which is an example of a ductile phase toughened molybdenum silicide. In Mo-Si-B alloys, the fracture toughness is expected to increase as the Mo-content is increased. On the other hand, to obtain some degree of oxidation resistance, relatively high Si and B concentrations (e.g. Mo–14Si–10B [12]) are required. However, ingots with high Si and B concentrations tended to have macroscopic cracks and were therefore not suitable for mechanical testing. The composition Mo–12Si–8.5B was chosen because its Si and B concentrations are low enough to permit casting without a significant density of macrocroscopic cracks.

[1] Unless stated otherwise, compositions will be given in at.%.

2. Experimental procedure

Alloys with the composition Mo–12Si–8.5B (at.%) were prepared by arc-melting in a partial pressure of argon (70 kPa) from high purity elements. The elemental Mo, Si, and B were 99.95, 99.99 and 99.5 wt.% pure, respectively. After melting several times on a water-cooled copper hearth, the alloys were dropped into a cylindrical water-cooled copper mold with a diameter of 25 mm and a length of 50 mm. The ingots were subsequently homogenized in vacuum (10^{-4} Pa) for 24 h at 1600°C. Some ingots destined for extrusion were dropped into MgO molds in order to reduce their cooling rates.

Several Mo–Si–B ingots were inserted into molybdenum extrusion cans with an outer diameter of 50 mm, which were evacuated and sealed by electron beam welding. The sealed cans were extruded through zirconia-coated H13 steel dies with an inner diameter of 25 mm at temperatures ranging from 1450 to 1600°C.

For the powder-metallurgical processing, arc-cast ingots of Mo_3Si and Mo_5SiB_2 were crushed into −100 mesh (< 150 μm diameter) powders. These powders were then mixed with appropriate amounts of 2–8 μm Mo powders and sealed in an evacuated Nb can, which was subsequently hot isostatically pressed (HIPed) for 1 h at 1650°C and 200 MPa.

Microstructural analysis was carried out by optical metallography and scanning electron microscopy (SEM) of polished specimens etched with Murakami's etch (an aqueous solution of potassium ferricyanide and sodium hydroxide). Phases were identified by powder X-ray diffraction and by measuring the Mo to Si ratio by energy-dispersive spectroscopy (EDS) in the SEM. Phase volume fractions were determined by full pattern fitting (Rietveld refinement) of the powder X-ray diffraction patterns [13].

A powder-metallurgical specimen was also examined by transmission electron microscopy (TEM). Specimens were prepared by mechanical dimpling to approximately 30 μm thickness followed by ion milling. Final thinning was carried out on a cryogenic stage using 8 kV argon ions until perforation occurred.

Flexure specimens with a cross section of 3×4 mm and a length > 20 mm were electro-discharge machined and ground, and subsequently tested in a screw-driven testing machine in a three-point bend fixture with a 20 mm span at different temperatures in air. It should be pointed out that, generally, three-point fracture strengths tend to be higher than four-point fracture strengths. The cross-head speed in all tests was 10 μm/s. Fracture toughness values were determined by three-point bend tests using chevron-notched specimens. The advantage of using such specimens is the relatively small amount of material required. The specimens were 3 mm wide and 4 mm high with a notch tip depth of 2 mm resulting in a

notch tip angle of approximately 75°. During testing, a crack initiated at the tip of the chevron-notch and propagated gradually through the specimen until fracture occurred. Fracture toughness values were determined based on an energy criterion by integrating the load-displacement curves. The fracture toughness was determined as $G = W/A$, where W is the energy absorbed during the fracture of the area A swept out by the crack. Assuming the material to be linear elastic, the fracture energy (energy criterium) can also be expressed in terms of the stress intensity (stress criterium) by $K_q = (G \times E')^{1/2}$, where $E' = E/(1-\nu^2)$ is the plane strain Young's modulus and ν is Poisson's ratio. Representative values for A and W were 2.8 mm^2 and 1 mJ, respectively.

High temperature tensile tests were carried out in flowing nitrogen using frictionally loaded miniature specimens [14]. The overall specimen and gage lengths were 25 mm and 6 mm, respectively, and the cross section was 2.5×2 mm. The specimens were held in TZM grips, and their elongation was measured by a precision transducer attached to the loading train. The tensile tests were conducted with loading rates of 0.04 and 1.0 μm/s.

3. Results and discussion

3.1. Cast and annealed Mo–12Si–8.5B (at.%)

3.1.1. Microstructure

A Mo–12Si–8.5B alloy was cast and annealed for 1 day at 1600°C in vacuum. Table 1, which includes data for the powder-metallurgical alloy to be discussed later, shows that the cast alloy had a low carbon and oxygen content. X-ray powder diffraction verified the presence of α-Mo, Mo_3Si, and Mo_5SiB_2. Fig. 2 shows that the α-Mo formed isolated particles in the Mo_3Si/Mo_5SiB_2 matrix. Table 2 shows the phase volume fractions calculated from the nominal composition Mo–12Si–8.5B by assuming the 3 phases to be pure Mo, and stoichiometric Mo_3Si and T2. The volume fractions of the 3 phases were also determined by Rietveld analysis [13] of a powder diffraction pattern (Table 2). According to the Rietveld analyis, the α-Mo contained approximately 1.2 at.% Si and 1.2 at.% B. The Si concentration agreed well with the EDS concentration determined by using Mo_3Si or T2 as standards, namely, 1.3 at.%. However, since the overall composition derived from the Rietveld analysis was Mo–12.4Si–9.4B, the Rietveld analysis appears to underestimate the α-Mo volume fraction. A 5–10% error in the Rietveld analysis is possible because of uncertainties in the peak profile function.

Table 1
Carbon and oxygen contents of cast and PM Mo–12Si–8.5B alloys

Processing route	Carbon, wt.ppm	Oxygen, wt.ppm
Casting	127	172
Powder-processing	35	697

3.1.2. Mechanical properties

The elastic constants were determined ultrasonically ($E = 327$ GPa and $\nu = 0.29$). The fracture toughness values calculated with these elastic constants are shown in Table 3. A comparison with more precise work by Choe and Ritchie [15] shows that the chevron-notch technique appears to overestimate the fracture toughness

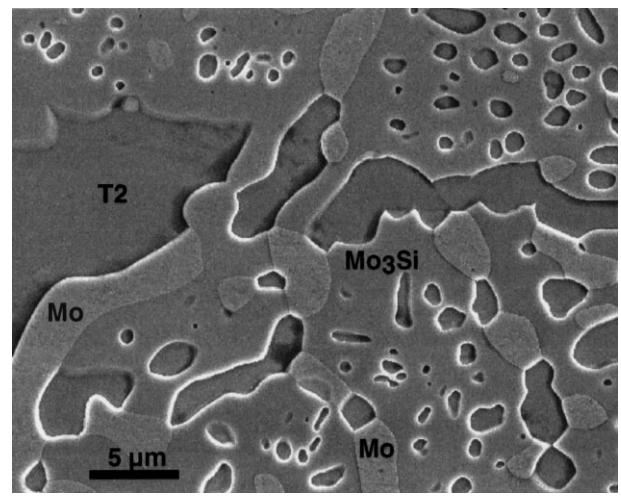

Fig. 2. SEM micrograph of polished and etched section of annealed Mo–12Si–8.5B.

Table 2
Volume fractions of the phases in Mo–12Si–8.5B

	Mo	$Mo_{0.75}Si_{0.25}$	$Mo_{0.625}Si_{0.125}B_{0.25}$ (T2)
Density, Mg/m^3	10.22	8.97	8.81
Molar volume, mm^3	9386.8	8802.7	7508.4
Average molar mass	95.94	78.976	66.176
Rietveld analysis	34.4	32.0	33.6
Calculated from nominal composition	38.4	31.8	29.8

Table 3
Three-point flexure strengths and fracture toughness values of cast and annealed (1 day/1600°C/vacuum) Mo–12Si–8.5B

Temperature, °C	Flexure strength, MPa	G, J/m^2	K_q, MPa m$^{1/2}$
20	484	231.0	9.1
20	539	269.5	9.8
500	722	271.0	9.8
500	697	361.7	11.4
1200	428	1312	21.6
1200	553	965	18.5

K_{Ic} by approximately 25%. Therefore, the fracture toughness values in this work were designated as K_q rather than K_{IC}. At room temperature, K_q is on the order of 10 MPa $m^{1/2}$. This value is significantly higher than the 3.3 MPa $m^{1/2}$ found for powder-processed Mo_3Si-50 wt.% T2 (which contains no α-Mo) [16]. The α-Mo causes therefore significant ductile-phase toughening. Generally, ductile phase toughening increases as the volume fraction and the size of the toughening phase increase [17]. However, since the mechanical properties of the α-Mo solid solution in Mo–12Si–8.5B are not known, a quantitative analysis was not performed. The as-cast alloy had values on the order of 7 MPa $m^{1/2}$. The lower fracture toughness of the as-cast material may be due to the smaller size of the toughening α-Mo particles. Also, the Si and B concentrations in the α-Mo in the as-cast alloy are likely to be higher and may compromise the toughening contribution of the α-Mo. An SEM micrograph of the room temperature fracture surface of an annealed specimen (Fig. 3) shows evidence for debonding and limited ductility of the α-Mo particles in the alloy. The 1200°C fracture toughness is considerably higher than that at room temperature or 500°C. This increase may be due to the high ductility of α-Mo at 1200°C, as well as limited ductility of Mo_3Si and T2.

Three-point flexure strengths were determined at three different temperatures in air (Table 3). The significantly higher strength at 500°C, as compared to room temperature, may be due to the increased ductility of the α-Mo phase at 500°C and the associated reduction in notch sensitivity of the specimen. The alloy retained a reasonably high strength at 1200°C. At 1200°C and loads near the fracture load, the load-displacement curves showed a slight deviation from linear elastic behavior, suggesting a small degree of plasticity (Fig. 4). In tensile tests in flowing nitrogen at 1200°C, on the other hand, no evidence for plasticity was observed and fracture took place in a brittle manner. The premature fracture may have been caused by bending moments during the tensile testing. However, with a combination of increased temperature (1520°C) and reduced loading rate (0.04 μm/s or 7×10^{-6} s^{-1}, respectively), a small amount of plasticity was observed. The loading curve in Fig. 5 indicates a plasticity-related deviation at about 195 MPa and brittle fracture at about 315 MPa. Assuming that the plastic elongation occurred only in the gage section, the plastic strain was only about 0.4% in spite of the very high testing temperature. SEM examination showed significant ductility of the α-Mo particles. The α-Mo was also very ductile at 1200°C and a strain rate of 1 μm/s as illustrated in Fig. 6. The relatively brittle behavior of Mo–12Si–8.5B even at very high temperature is therefore attributed to the brittleness of the intermetallic phases Mo_3Si and T2.

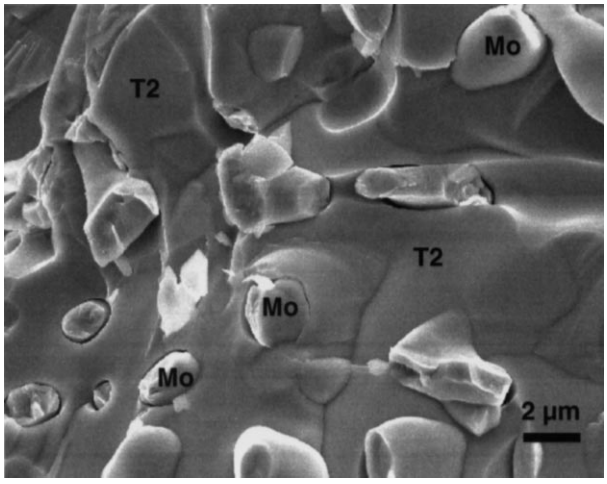

Fig. 3. SEM micrograph of room temperature fracture surface illustrating debonding and slight ductility of the α-Mo in annealed Mo–12Si–8.5B.

3.2. Hot extrusion of cast alloys

Extrusion of Mo–Si–B alloys was attempted to refine the microstructure and reduce or eliminate micro- or macro-cracks formed during casting. Two Mo–12Si–8.5B ingots cooled in Cu molds were canned in Mo. Extrusion at 1450°C was aborted because the load capacity of the press was reached once the Mo near the nose of the can had extruded. A second extrusion attempt with a glass lubricant at 1550°C proceeded to completion. However, the alloy was severely cracked. Slowly cooled ingots (MgO mold) with the composition Mo–14Si–10B were also extruded at 1600°C, but the extruded product was again severely cracked. Research carried out at Universal Energy Systems (UES) is in qualitative agreement with our results [18]. In that work, a cast silicide with the composition Mo–12Si–12B was extruded at 1800°C. Again, the extruded material was heavily cracked. Clearly, sound extrusions of cast Mo–Si–B alloys containing substantial volume fractions of Mo_3Si and T2 are difficult to achieve. Mo_3Si and T2 appear to be brittle at high strain rates even when the temperature is very high. Similar difficulties were previously reported for an alloy with the composition Mo–26.7Si–7.3B consisting of Mo_5Si_3, Mo_3Si, and T2 [19].

4. Powder-metallurgical Mo–12Si–8.5B alloys

A powder-metallurgical (PM) specimen with the nominal composition Mo–12Si–8.5B was prepared in the following manner: arc-cast ingots of Mo_3Si and T2 were pulverized into -100 mesh (< 150 μm) powders. These powders were mixed with 2–8 μm Mo powder and sealed in an evacuated Nb can, which was subsequently hot isostatically pressed (HIPed) for 1 h at 1650°C and 200 MPa. The HIPed material had a low carbon content and, as expected, a relatively high oxygen

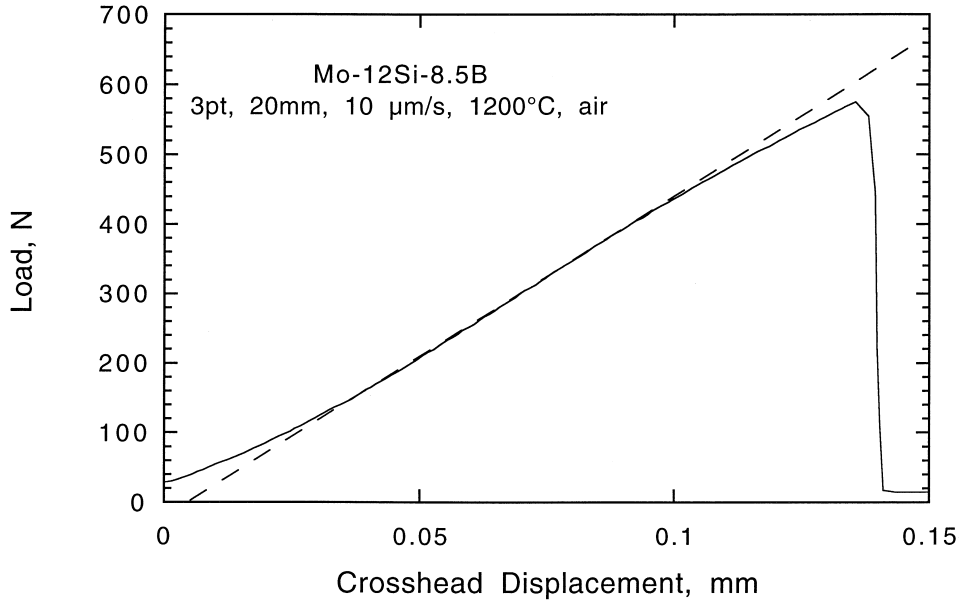

Fig. 4. Load-displacement curve for Mo–12Si–8.5B deformed in 3-point flexure at 1200°C in air.

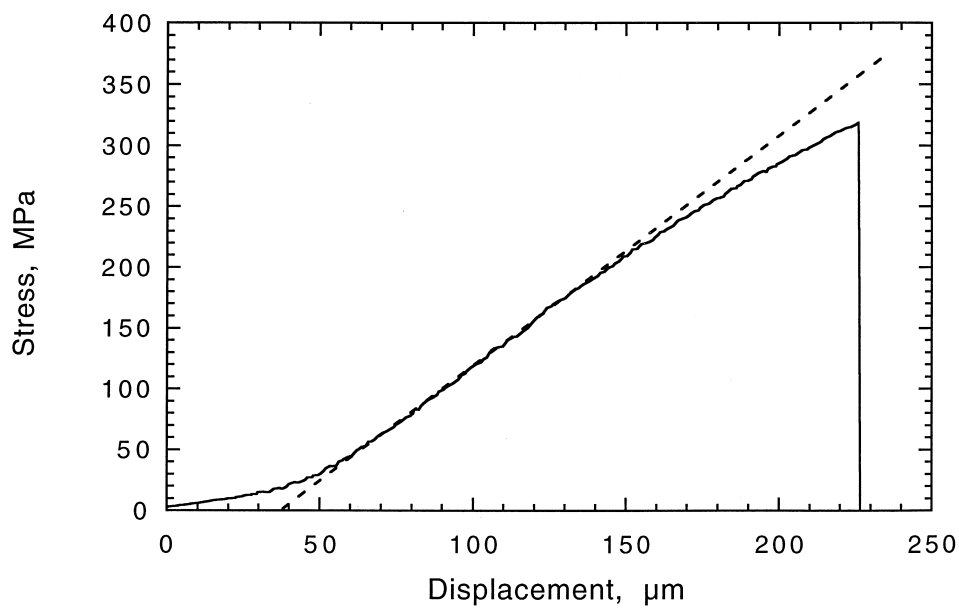

Fig. 5. Tensile stress-strain curve of Mo–12Si–8.5B strained at 1520°C with a crosshead speed of 0.04 μm/s.

content (Table 1). A back-scattered SEM micrograph (SEM) of a polished and etched specimen is shown in Fig. 7. The large intermetallic particles were often cracked. Whereas the corresponding cast material contained α-Mo particles in a brittle matrix, the PM material consisted of intermetallic particles embedded in an α-Mo matrix. The dark spots in the α-Mo contained Si and O (B could not be analyzed by EDS) and are probably borosilicate glass. The brightest phase with the highest mass contrast is α-Mo. T2 can be distinguished from Mo_3Si by the etching contrast at the periphery of T2.

Transmission electron microscopy showed that, locally, the microstructure was free of SiO_2. In particular, no evidence was found for silica films at the interphase boundaries, which would reduce the high-temperature creep strength. The SiO_2 appeared to occur in the microstructure in the form of isolated particles or clusters. The three crystalline phases were identified by a combination of X-ray spectroscopy and selected area diffraction. TEM images of the α-Mo phase showed fine black speckles (a few nm in size) which were attributed to radiation damage from the ion milling. None of the

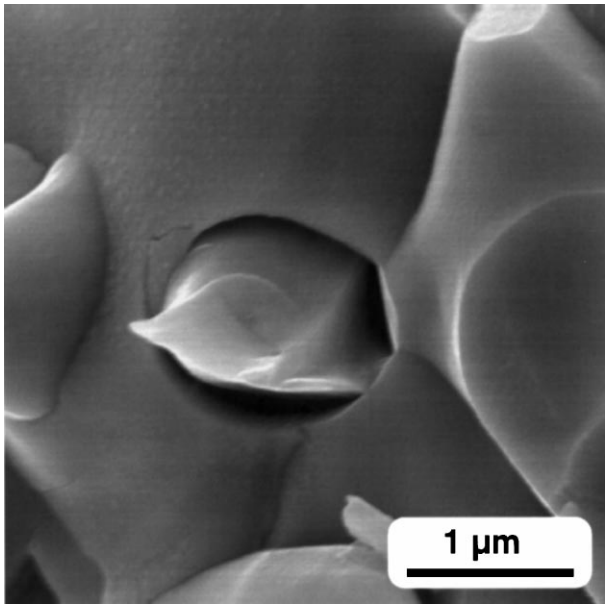

Fig. 6. SEM micrograph of the fracture surface of a tensile Mo–12Si–8.5B specimen which failed at 1200°C in a brittle manner.

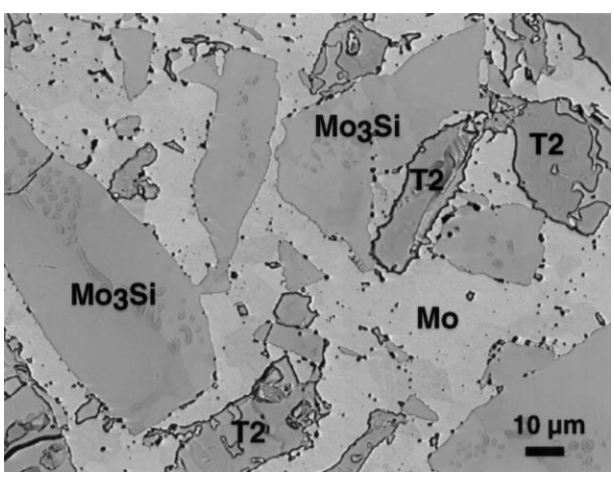

Fig. 7. Back-scattered SEM micrograph of Mo–12Si–8.5B hot isostatically pressed from Mo_3Si, T2, and Mo powders.

Table 4
Mechanical properties of PM material with the nominal composition Mo–12Si–8.5B

Room temperature flexure strength, MPa	Room temperature fracture toughness, MPa $m^{1/2}$
384	14.0
376	15.6
412	
408	

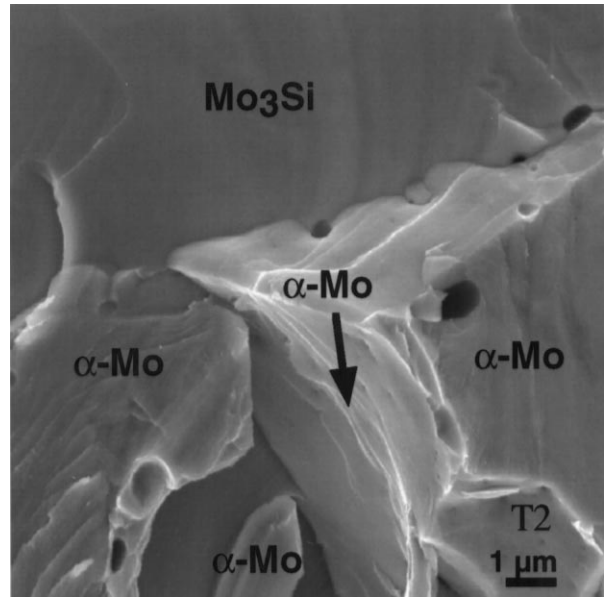

Fig. 8. Room temperature fracture surface of PM Mo–12Si–8.5B.

intermetallic phases showed signs of radiation damage. The few dislocations found were in the α-Mo or T2 phases and were typically associated with small inclusions or arranged into low angle boundaries.

Table 4 shows the room temperature flexure strength and fracture toughness of PM Mo–12Si–8.5B. Due to the high density of cracks it is not surprising that its strength is lower than that of cast and annealed material with the same nominal composition (compare Table 1). Its fracture toughness, on the other hand, is distinctly higher. There are three reasons for this. First, the microstructure consists of a continuous α-Mo matrix instead of individual α-Mo particles. This type of structure is similar to that of cemented tungsten carbide. In particular, a propagating crack cannot avoid the toughening α-Mo. The ridge indicated by the arrow in Fig. 8 shows some evidence for plastic deformation of the α-Mo on a room temperature fracture surface (although not as clearly as for the α-Mo on the fracture surface in Fig. 3). The PM processing did therefore not unduly embrittle the Mo. Second, the microstructure in the PM material is much coarser than that in the cast and annealed alloys, and it is well known that coarse microstructures result in higher ductile-phase toughening than fine microstructures [17]. Third, the processing-induced cracks and pores in such brittle materials typically increase the fracture toughness since they dissipate local strain energy through additional microcracking during fracture. No further mechanical testing has been carried out for this PM material, since its processing needs to be improved to eliminate microcracks. However, due to its continuous α-Mo matrix, the PM material has the potential for higher ductility and fracture toughness than the corresponding cast material, which consists of a continuous brittle matrix.

5. Summary and conclusions

Cast and annealed molybdenum silicides with the composition Mo–12Si–8.5B consist of α-Mo particles in a matrix of Mo_3Si and T2. They exhibit room temperature fracture toughness values on the order of 10 MPa $m^{1/2}$. These relatively high values are consistent with the observed debonding and deformation of the α-Mo particles observed on fracture surfaces. Even at temperatures as high as 1200°C substantial flexure strengths on the order of 400–500 MPa were observed. Hot extrusion of cast Mo–12Si–8.5B was unsuccessful since the extruded material was cracked severely. Microstructures containing Mo_3Si and T2 particles in a α-Mo matrix were obtained by powder-metallurgical processing. Because of the coarse microstructure, and because of the inability of the cracks to avoid ductile α-Mo particles, these microstructures were associated with significantly improved room temperature fracture toughness values. Such PM materials offer potentially more ductility than the corresponding cast and annealed materials.

Acknowledgements

This research was sponsored by the Office of Fossil Energy, Advanced Research Materials (ARM) Program, U.S. Department of Energy, under contract DE-AC05-00OR22725 with Oak Ridge National Laboratory, managed by UT-Battelle, LLC. The work at Ames Laboratory was supported by the Advanced Energy Project (AEP), U.S. Department of Energy under contract No. W-7405-Eng-82 with Iowa State University. The considerable help of C. A. Carmichael with the alloy preparation is appreciated.

References

[1] Hebsur MH. Development and characterization of $SiC_{(f)}/MoSi_2$–$Si_3N_{4(p)}$ hybrid composites. Mat Sci Eng 1999;A261:24–37.
[2] Nowotny H, Kimakopoulou E, Kudielka H. Untersuchungen in den Dreistoffsystemen: Molybdän-Silizium-Bor, Wolfram-Silizium-Bor und in dem System: VSi_2-$TaSi_2$. Mh Chem 1957;88:180–92.
[3] Nunes CA, Sakidja R, Perepezko JH. Phase stability in high temperature Mo–rich Mo–B–Si alloys. In: Nathal MV, et al, editors. Structural intermetallics. Warrendale (PA): TMS, 1997. p. 831–9.
[4] Huebsch JJ, Kramer MJ, Zhao HL, Akinc M. Solubility of boron in $Mo_{5+y}Si_{3-y}$. Intermetallics 2000;8:143–50.
[5] Meyer M, Kramer M, Akinc M. Boron-doped molybdenum silicides. Adv Mater 1996;8:85–8.
[6] Meyer MK, Kramer MJ, Akinca [sic] M. Compressive creep behavior of Mo_5Si_3 with the addition of boron. Intermetallics 1996;4:273–81.
[7] Meyer MK, Thom AJ, Akinc M. Oxide scale formation and isothermal oxidation behavior of Mo-Si-B intermetallics at 600–1000°C. Intermetallics 1999;1000(7):153–62.
[8] Berczik DM. United States Patent 5,595,616 (1997). Method for enhancing the oxidation resistance of a molybdenum alloy, and a method of making a molybdenum alloy.
[9] Berczik DM. United States Patent 5,693,156 (1997). Oxidation resistant molybdenum alloy.
[10] Perepezko JH, Nunes CA, Yi S-H, Thoma DJ. Phase stability in processing of high temperature intermetallic alloys. In: Koch CC, et al, editors. High-temperature ordered intermetallic alloys. Warrendale (PA): MRS, 1996. p. 3–14.
[11] Sakidja R, Sieber H, Perepezko JH. Microstructural development of Mo–rich Mo–B–Si Alloys. In: Crowson A, Chen ES, Shields JA, Subramanian PR, editors. Molybdenum & Molybdenum Alloys Warrendale (PA): TMS, 1998. p. 99–110.
[12] Schneibel JH, Liu CT, Easton DS, Carmichael CA. Microstructure and mechanical properties of Mo-Mo_3Si-Mo_5SiB_2 silicides. Mat Sci Eng 1999;A261:78–83.
[13] Larson AC, Von Dreele RB. General structure analysis system, Los Alamos National Laboratory report LAUR 86-748, Los Alamos, NM, 1994.
[14] Ünal Ö. High temperature tensile and creep properties of Mg-Y alloys. In preparation.
[15] Choe H, Ritchie RO, Lawrence Berkeley National Laboratory, in preparation.
[16] Schneibel JH, Lin HT. Processing and properties of molybdenum silicide intermetallics containing boron. In: Judkins RR, editor. Proceedings 14th Annual Conference on Fossil Energy Materials, Oak Ridge National Laboratory, 24–26 April, 2000.
[17] Ashby MF, Blunt FJ, Bannister M. Flow characteristics of highly constrained metal wires. Acta Metall 1989;37:1847–57.
[18] Mendiratta MG, personal communication, 1999.
[19] Schneibel JH, Liu CT, Heatherly L, Kramer MJ. Assessment of processing routes and strength of a 3-phase molybdenum boron silicide (Mo_5Si_3–Mo_5SiB_2–Mo_3Si). Scr Mater 1998;38:1169–76.